

Study of young stellar objects and associated filamentary structures in the inner Galaxy

B Bhavya^{1*}, Annapurni Subramaniam^{2†}, V C Kuriakose¹

¹Department of Physics, Cochin University of Science & Technology, Kochi 682 022, India

²Indian Institute of Astrophysics, Bangalore 560034, India

11 September 2018

ABSTRACT

Young Stellar Objects (YSOs) in the inner Galactic region $10^0 < l < 15^0$ and $-1^0 < b < 1^0$ are studied using GLIMPSE images and GLIMPSE data catalogue. A total number of 1107 Class I and 1566 Class II sources are identified in this Galactic region. With the help of GLIMPSE $5.8 \mu\text{m}$ & $8 \mu\text{m}$ images, we have identified the presence of 10 major star forming sites in the Galactic midplane, of which 8 of them are filamentary while 2 are possible clusters of Class I & II sources. The length of the identified filaments are estimated as $8' - 33'$ ($\sim 9 - 56 \text{ pc}$). Occurrence of Hub-Filamentary System (HFS) is observed in many filamentary star forming sites. Most of the Class I sources are found to be aligned along the length of these filamentary structures, while Class II sources have a random distribution. Mass and age distribution of 425 Class I and 241 Class II sources associated with filaments & clusters are studied through their SED analysis. Most of the Class I sources detected have mass $> 8M_{\odot}$, while Class II sources have relatively low mass regime. Class I sources have ages $\leq 0.5 \text{ Myr}$, while Class II sources have ages in the range $\sim 0.1 - 3 \text{ Myr}$. Along with the help of high mass star forming tracers, we demonstrate that the 10 regions studied here are forming a large number of high-mass stars.

Key words: stars: formation, stars: pre-main-sequence, infrared: stars

1 INTRODUCTION

Star formation processes in the inner Galactic regions are important to understand as it happens in an environment of relatively higher density and metallicity. Apart from that these are sites where high mass star formation happens vigorously. It is interesting to see that the galactic region from $10^0 < l < 15^0$ nurtures many features like filamentary structures, bubbles, HII regions which are observed only at longer wavelengths indicating that the region is highly dynamic, active and young in nature. Heavy obscuration of visible light blocks the study of inner galaxy using optical wavelengths. Owing to its high sensitivity and angular resolution, *Spitzer* (Werner et al. (2004)) revolutionized our view of inner galaxy and enabled us to detect features which were not previously identified using optical wavelengths. The results are far reliable and accurate compared to previous poor resolution far-IR and millimeter observations. Mid Infra-Red (MIR) observations, which are less affected by dust extinction compared to near-IR and optical wavelengths, done with Infra Red Array Camera (IRAC) of *Spitzer* (Fazio et al. 2004) lead a deeper understanding of early star formation scenario. The Galactic midplane which comprises the major sites of massive star formation is mapped with Science Legacy Program GLIMPSE

surveys. GLIMPSE I (Benjamin et al. 2003) survey imaged the inner Galaxy from longitudes $l=10^0$ to 65^0 and latitude $|b| \leq 1^0$ with resolution $< 2''$ in all IRAC bands.

Relative to the low-mass star formation processes, the high mass star formation mechanism is poorly understood. Some of the reasons for the paucity of such studies are: high mass stars have a short pre-main sequence time scale, most of the high-mass star forming regions are distant, difficulty in observing earliest stages of high-mass star forming processes, difficulty in getting a bonafide sample of high-mass stars, highly embedded nature of massive star forming sites make them difficult to resolve and locate. Hence, it has been difficult to characterize high-mass ($\geq 8M_{\odot}$) star forming processes. Understanding high mass protostars are highly essential in the study of universal initial mass function. In this paper, we present a study of star forming regions at low Galactic latitudes. This region is suggested to be undergoing high mass star formation as revealed by previous studies. The region of our interest is the inner Galactic plane, in the longitude-latitude range, $10^0 < l < 15^0$ and $-1^0 < b < 1^0$, and close to M17, W33 and W31 star forming regions. This region is located to the south-west of M17 which harbors many features which are not detectable in optical, but shows prominent features in longer wavelengths including mid-IR. CO map given by Sanders et al. (1986) shows the presence of molecular clouds in this region. Several regions in this longitude-latitude range have been previously studied by others. Many of the studies

* E-mail: bhavyab@cusat.ac.in

† E-mail: purni@iiap.res.in

are based on the HII region complexes such as, W31 (G10.2-0.3 & G10.3-0.1) (Wilson 1974, Caswell et al. 1975, Corbel & Eikenberry 2004, Kim & Koo 2002, Furness et al. 2010, Beuther et al. 2011) and W33 (Goss et al. 1978, Soifer et al. 1979, Stier et al. 1982, Goldsmith & Mao 1983, Haschick & Paul 1983, Messineo et al. 2011) and also other ultra compact HII regions, G10.6-0.4 (Persson et al. 2012, Gerin et al. 2010, Neufeld et al. 2010, Klassen et al. 2011, Liu et al. 2011, Sollins et al. 2005), G10.47+0.03 (Roloffs et al. 2011, Pascucci et al. 2004, Olmi et al. 1996), G10.62-0.38 (Beltran et al. 2011) etc. High mass star formation in the infra-red dark cloud G11.11-0.12 (Region 9 in our study), which is at a kinematic distance of 3.6 kpc (Clemens et al. 1986), has been studied using water and methanol masers by Pillai et al. (2006), using Herschel data by Henning et al. (2010) and more recently by Gomez et al. (2011). Though all the above regions are located in the first galactic quadrant covering the near 3-Kpc arm, studies do not discuss their connection with the 3-Kpc arm. According to Downes et al. (1980) W31 complex is a part of 3-Kpc arm, while Dame & Thaddeus (2008) find that the velocity peaks of W31 are not in accordance with the general 3-Kpc arm kinematics. The detection of ultra compact HII regions implies the primitive nature of this region. This might suggest that a large amount of molecular cloud in the inner galaxy is triggered to form stars, similar to "global triggering", as indicated by Povich & Whitney (2010) in the case of M17SWex. This region is a part of several surveys like CO maps, methanol masers, infra red dark clouds (IRDCs), star-less clumps, HII regions etc. We have used the results from some of the previous surveys as tracers of high mass star formation and to resolve the uncertainty in distance towards these regions.

Elongated structures of parsec scales seen in star forming complexes have been extensively studied by Myers (2009), who analyzed the general properties of elongated structures observed in deep optical, near-IR, CO mapping, IRAC and GLIMPSE/MIPSGAL images. According to which, a "hub" is termed as a central blob of high column density, with peak column density $10^{22-23} \text{ cm}^{-2}$ and filament denotes associated feature of low-column density. Smaller hubs tend to be relatively round, with fewer stars, lower column density and with a few radiating filaments. Larger hubs are more elongated, with more stars, higher column density and with 5-10 filaments. These filaments are nearly parallel to each other, directed along the short axis of the hub, with similar spacing and direction forming a "hub-filamentary system" (HFS). HFS is seen in dust emission and absorption, and in molecular line emission. It is seen in optical dark clouds within a few hundred pc, and in IRDCs at distances ~ 3 kpc. In this region, we notice filamentary features, with a few showing HFS.

Here we make use of the point-source catalog and image cut-outs from GLIMPSE I survey to demonstrate the young stellar content and features in the inner galactic mid-plane. The YSO spectral energy distribution deviates at mid-IR wavelengths from normal photospheric emission. The Spitzer-IRAC sensitivity to mid-IR emission makes it the best tool to identify and characterize YSOs. Sources with excess mid-IR emission are classified as Class I (still embedded and accreting from dense spherical envelopes) and Class II (slightly more evolved pre-main sequence stars with circumstellar disks) (Lada et al. 2006, Gutermuth et al. (2008)). The mass and the age range of YSOs in each region are estimated and used to understand the ongoing star formation and the filamentary structure.

This paper is structured as follows. Section 2 describes the archival data catalogues we used for the study of galactic central

regions. In Section 3 we detail the analysis and results, which includes Classification of IRAC sources, Spectral Energy Distribution fitting for the YSOs, Identification of Filamentary structures & Clustering with its descriptions, Spatial distribution of YSOs and tracers of high-mass star formation. In Section 4 we include a brief discussion and summarize our main findings in section 5.

2 ARCHIVAL DATA CATALOGUES USED FOR THIS STUDY

In order to understand the details of star formation in the region of interest, we combine the following archival data with the YSOs identified in this study. As these sources are tracers of high mass star formation, these will be used to compare the masses and ages of the YSOs studied here. Since we do not have any distance estimate towards the YSOs studied here, we use the distance estimate for the sources in the archival data to obtain a possible range of distance to the YSOs. As some of the sources are mentioned in the literature to be associated with the inner spiral arms of the Galaxy, we combine this information to connect the features identified in this study with the spiral structure of the inner Galaxy.

Infra Red Dark Clouds (IRDCs):

IRDCs, which appear as silhouettes in the general galactic mid-IR background are the precursors of cluster forming molecular clumps (Carey et al. 1998, Jackson et al. 2008) and IRDC cores host the very earliest phases of high mass star formation (Rathborne et al. 2005, Rathborne et al. 2006, Rathborne et al. 2007, Simon et al. 2006). We have taken the catalogue from Peretto & Fuller (2009) which provides a complete sample of IRDCs in the galactic range $10^0 < |l| < 65^0$ and $|b| < 1^0$ using GLIMPSE and MIPSGAL survey.

Methanol Masers:

According to Green et al. (2009), the Methanol maser transition at 6.7 GHz have been observed towards early hot core phases of star formation processes and found to be associated with tracers of high mass star formation in IRDCs (Ellingsen 2006) and Extended Green Objects (EGOs) (Cyganowski et al. (2008)). Using Methanol Multibeam (MMB) Survey, Green et al. (2009) and Green et al. (2010) conducted a search for methanol masers and showed that significant star formation is happening in the 3-Kpc arm, which is existing within the 15^0 of Galactic center. MMB detected more than 200 methanol masers in the region $15^0 < l < -15^0$ and 49 of them have velocity peak matching that of near and far 3-Kpc arms. Among them 52 sources are located in our region of interest, of which, 4 sources are identified as 3-Kpc arm signatures and 2 sources as far arm features by Green et al. (2010).

Star-less clumps:

Using ATLASGAL survey at $870 \mu\text{m}$, Tackenberg et al. (2012), made a search for dense gas condensations. Along with GLIMPSE catalogue and $24\mu\text{m}$ MIPSGAL images, this survey showed the existence of starless cores which may form high mass stars, in the galactic region $10^0 < l < 20^0$ and $|b| < 1^0$. The catalogue also provides distances (both far and near) towards these objects.

IR bubbles/HII regions:

IR bubbles, as being the most spectacular objects in the GLIMPSE/MIPSGAL images, are the HII regions produced by radiation and wind from O and early B type stars of age $\sim 10^6$ yr (Churchwell et al. 2009) and therefore located at sites of recent massive star formation. Anderson et al. 2011 presents the catalogue of HII regions in the galactic region $343^0 \leq l \leq 67^0$ and $|b| \leq 1^0$.

Radio sources:

Galactic radio sources are taken from radio continuum survey (CORNISH survey) by Purcell et al. (2013), targeting UCHIIIs in high mass star formation. CORNISH project covers northern GLIMPSE region ($10^0 < l < 65^0$) using the Very Large Array at 5 GHz. We identified 10 such radio sources to be located in our $l - b$ range.

We also show the location of 2 high mass protostellar objects (HMPOs) from Grave & Kumar (2009) and Extended Green Objects (EGOs) as tracers of massive young stellar objects (MYSOs) from Cyganowski et al. (2008), (4 'likely' MYSO outflows and 1 'possible' MYSO outflow), situated in our region of study. The spatial association of these sources (mainly as tracers of high mass star formation) and YSOs identified in our analysis will be discussed in later sections.

3 ANALYSIS & RESULTS

3.1 Classification of IRAC sources

More than 5 million sources from GLIMPSE I survey in the longitude-latitude range $l = 10^0 - 15^0$; $-1^0 < b < 1^0$ are examined to identify candidate YSOs. As only Spitzer-IRAC magnitudes are used in the identification of YSOs, in order to improve the reliability, we have taken only those IRAC sources with error less than 0.1 mag in all IRAC bands. The contamination from non-YSO sources and the effect of reddening are to be eliminated to create a bonafide sample of YSOs. We follow the Gutermuth et al. 2009 (hereafter G09) procedure to remove background contamination and to select Class I and Class II sources. Brief outline of 5 steps in identifying YSOs are described here.

G09 proposed an empirical scheme for identifying and classifying YSOs on the basis of mid-IR magnitudes and colors eliminating possible contaminants. According to Stern et al. (2005), galaxies dominated by PAH emission (normal star-forming galaxies) show excess in $4.5 \mu\text{m}$ and $5.8 \mu\text{m}$ band passes and broad line AGNs, having non stellar spectral energy distributions, exhibit MIR color indices similar to YSOs. Only very few (3) PAH emission sources and no AGN sources are identified in our sample by giving respective color cuts based on G09.

The high velocity outflows from protostars colliding with surrounding molecular cloud cause unresolved blobs of shock emission and are sensitive to the $4.5 \mu\text{m}$ IRAC band as it covers molecular hydrogen emission lines. By giving G09 constraints in the $[4.5]-[5.8]$ Vs $[3.6]-[4.5]$ color space, we detect 19 sources as shock emission sources and are removed. Additional contaminants are spurious excess emission in the $5.8 \mu\text{m}$ and $8.0 \mu\text{m}$ band passes caused by PAH emission sources, which contaminate the photometric apertures of some faint field stars. There were 13563 of such contaminants.

After removing the above mentioned contaminants, sources which satisfy the conditions of protostellar colors are classified as Class I sources. Figure 1(*Left*) shows the Class I sources (red triangles), other contaminants such as shock emission sources (blue) and PAH aperture contaminants (green) and the unclassified remaining sources (black). First these Class I sources are extracted. Later, from the remaining sources, those with consistent colors of pre-main sequence stars having circumstellar disk are classified as Class II sources. Figure 1(*Right*) shows Class II sources (red) and unclassified sources (black) which mostly contain stars close to main sequence. There are 1107 Class I sources and 1566 Class II sources identified in the region of interest. GLIMPSE catalog also provides 2MASS magnitudes for these sources. All these

sources have 2MASS magnitudes, but only 103 Class I and 1090 Class II sources have 2MASS magnitudes with error less than 0.1 mag. We have not de-reddened IRAC colors. We caution that reddening can affect the the number of Class I&II sources identified. The extinction vectors (Flaherty et al. 2007) corresponding to $A_k=5$ mag are shown in the Figure 1. As our study does not aim to obtain a complete sensus of YSOs in this region, but understand the nature and location of early star formation, we do not attempt to achieve the completeness limit in detecting YSOs. Since an upper limit for the error in the IRAC magnitudes are set, our estimation of YSOs is a lower limit of the number of YSOs present in this location. Sources identified here are likely to be genuine detections and would help us to derive reliable properties of these sources as well the star formation sites.

We point out the caveats and drawbacks of this study. Since only those sources with sufficient flux in all IRAC bands are considered in this study, faint low-mass Class I&II sources, evolved Class II sources and distantly located sources will be missed. Reduced number of these sources in our study is due to the sample selection and not due to the absence of these sources in the region. There will also be source contamination from edge-on disk sources and reddened Class II sources which would mimic their colors as Class I sources. Gutermuth et al. (2009) gives an upper limit for the edge-on disk source confusion as $3.3 \pm 1.5\%$. Kryukova et al. (2012) showed that there will be 4% contamination due to edge-on sources in their YSO sample. We also assume a similar fraction of edge-on sources in our sample. The major impact of not using MIPS GAL data is that we are unable to identify reddened Class II sources.

In order to understand the distribution of these sources, the location of Class I and Class II sources in the region studied are shown in Figure 2. Location of M17, W31 and W33 are also shown. It can be seen that the Class I sources are found to be located as groupings, whereas the Class II sources are located all over the region. The class I sources are distributed very close to the galactic plane, except in the M17SWex region. Specific locations of Class I groups can be identified and found to coincide with the location of other tracers of high-mass star formation. The Class II sources do not show any preferential confinement to the galactic plane. They are distributed randomly in the region, except for a couple of clusters. Thus, the Class I sources are likely to be associated with the sites of high-mass star formation, most of which are located along the galactic plane in the $l-b$ range studied.

3.2 Filamentary structures and Hub-Filamentary System (HFS)

The $5.8 \mu\text{m}$ & $8 \mu\text{m}$ images from GLIMPSE reveal the presence of filamentary structures in the region, which appear as dark patches in mid and far IR images of the region. Close inspection of the images reveal several tiny filaments emanating from the main filament forming a hub-filamentary system (HFS). Class I sources are found to be aligned as a string along the length of these filamentary structures. We identify 8 such filamentary structures of star forming regions and 2 candidate clusters of Class I & Class II sources in the entire region, each of which will be described in detail in section 3.5. Filamentary structures are assumed to be primitive star forming sites; whereas the candidate clusters are slightly evolved. The location of these identified regions are marked in Figure 2. We have defined boxes to differentiate the filamentary regions & clusters from background. Though the sizes of the boxes do not limit the actual physical extent of each region, we have considered only those sources inside the boxes for further analysis. Size and shape

of the boxes which define the boundary of the regions are defined to include most part of the filamentary structure as seen in the images. We study the YSOs in these structures and correlate the location of Class I and II YSOs with the filamentary structures to get the nature of star formation they host. Though the Class II sources are randomly distributed in these regions (except for the regions near W33 and near M17SWex where we can see a preferential clustering of Class II sources), Class I sources are either clumpy or closely associated with the filaments. In the entire region, we detect more number of Class II sources, compared to the Class I sources, with a ratio of 0.7.

In all the filamentary regions, there is a higher concentration of Class I sources along the filaments. This can be due to either the reddened Class II sources appearing as Class I sources or intrinsically, Class I sources are more there. These filaments of dark clouds can be the precursors of massive star formation and progenitors of young clusters as noted by previous studies. The catalogue of IRDCs taken from Peretto & Fuller (2009) in the same l - b range is used to see whether the IRDCs and YSOs are co-located. When positional match is done between YSOs and IRDCs, their central coordinates do not match within 2'' separation. But we see the association of YSOs and IRDCs from 3'' separation onwards. In order to quantify the association of YSOs with the known IRDCs, we computed the distance of Class I/II sources from the IRDCs. The histogram (Figure 3) shows the summary of this estimate for all the IRDCs. Up to a distance of 90'' from IRDCs, the number of Class I sources are more than the number of Class II sources. Beyond this, the number of Class I and Class II sources are similar. Peretto & Fuller (2009) gives the physical extent of each of the IRDCs, which comes greater than 5'' (in the range 30''-50''; in some cases more than 200''). Hence, it can be assumed that at least some of the YSOs are associated with the same region where the IRDCs are also found. In general, wherever we find a high density of Class I sources, number of IRDCs are also found to be more. This once again proves that the filamentary regions identified here are probable sites of high mass star formation.

3.3 Distances

The region in southwest of M17, $9^{\circ} < l < 14^{\circ}$, $-0.2^{\circ} < b < -0.45^{\circ}$ is termed as 3-Kpc arm (Rougeot & Oort 1960, Clemens et al. 1986) which contains several molecular clouds; where the near 3-Kpc arm is at a distance of 5.2 kpc from Sun. Most of the star formation studies in the 3-Kpc arm are focused on the other end of the arm which extends in the l range $340^{\circ} - 360^{\circ}$ (4th Galactic quadrant). The association of the filamentary structures in our study to near 3-Kpc arm has been checked by comparing other studies in this region. In order to physically associate sources they have to be coherent in lbv space. The latitude range $10^{\circ} < l < 15^{\circ}$ meets several spiral arms as crossing over in the galaxy, the velocity measurements in this l range will give ambiguous results. Though our region of study is an extent of M17SWex in l - b space; it is more close to galactic plane (b is less compared to M17 and M17SWex). So we assume that this region is not physically associated with Sagittarius arm, but might be a part of other inner arms. M17 and M17SWex are at a distance of 2.1 kpc in the Sagittarius arm (Povich & Whitney (2010)). The previous distance estimations towards W31 and W33 star forming regions give a range of values (3.3 - 7 kpc towards W31 and 2.4 - 7 kpc towards W33). Keeping aside the distance ambiguity, the study of this region is of importance as it can give insights into initial states and characteristics of the formation of massive stars, OB associations and stellar clusters.

Since the uncertainty related to the distance exists for the identified sources in the entire region, while fitting SED, we have given a common distance range of 4-6 kpc in the input of SED fitting tool (except for regions 1 & 2 and for region 9 as 2.1 kpc (Povich & Whitney (2010)) and 3.6 kpc (Henning et al. (2010)) respectively, with a $\sim 10\%$ uncertainty in range (Table 1.).

3.4 Spectral Energy Distribution

In order to characterize the nature of YSOs, we construct spectral energy distributions (SEDs) for Class I and Class II objects identified in the filamentary regions and clusters. We follow the online YSO SED fitting tool developed by Robitaille et al. (2007) to estimate the physical properties such as mass, age, accretion rate of disks and envelopes of YSOs. In the Robitaille et al. (2007) models, masses are sampled between 0.1 to $50M_{\odot}$ and ages between 10^3 to 10^7 Myr. For each set of mass and age, temperature and radius are found by interpolating pre-main sequence evolutionary tracks of Seiss et al. (2000) and Bernasconi & Maeder (1996). Once the stellar parameters are determined, values of disk and envelope parameters are sampled from ranges that are functions of evolutionary age of the central source, as well as functions of stellar masses in certain cases. Parameters corresponding to the model which fits the observed flux values with χ^2_{min} are taken as the YSO parameters. Parameters of models which satisfy the criteria $\chi^2_{min} - \chi^2_{best} < 3$ where χ^2 is the statistical goodness of fit parameter per data point, are used to estimate the error in the estimated parameters.

SED analysis is carried out only for 425 Class I and 241 Class II sources which are detected within boundary of the 10 identified regions. We have assumed an A_v range of 1-40 mag for these sources. SEDs are constructed using 2MASS and IRAC magnitudes (wavelength range 0.1-8 μm) for some sources, whereas only IRAC magnitudes are considered for other sources. This is because, some YSOs have error more than 0.1 mag in the 2MASS magnitudes, which give unrealistic SED fittings. This means that for each region a few SEDs are made from IRAC and 2MASS magnitudes, whereas the remaining SEDs are constructed with IRAC magnitudes only. Figure 4 shows examples of SEDs of two Class I and two Class II YSOs from different regions. The solid black line shows the best-fitting model while the grey lines represent models which satisfy the above mentioned criteria. Among the output parameters, we present the results on mass and age estimates in the next section. The assumptions used in the models affect the reliability/accuracy of estimated parameters; which are considered as inevitable errors which occur in attempts of model dependent parameter estimations. The estimated parameters are based on the data mentioned above and do not include far-IR data. This introduces relatively large errors in the estimated parameters, as suggested by the large number of grey coloured fitted lines in the SED plots. Since Class I sources peak in mid-IR wavelengths, and Class II sources in NIR, mass and age estimations based on NIR and MIR are reliable to certain extent. In the absence of far-IR wavelengths, disk parameters are less constrained and the envelope parameters are highly uncertain. Inclusion of far-IR and sub-mm data will reinforce the disk nature and characteristics of YSOs. Results presented in this study are based on the high resolution data for a wide sample of candidate YSOs based on combined 2MASS and GLIMPSE data. The relatively poor resolution due to large aperture sizes of longer wavelength observations have to be addressed. Inclusion of longer wavelength data would effectively reduce the detected source density in each region, especially since these are distant star forming regions. Hence, instead of a statistical analy-

sis of the properties of large number of Class I/Class II sources, it would reduce to individual source studies.

3.5 Parameters of the identified YSOs

The number of Class I and Class II sources identified in each region are tabulated in Table 1, along with the number of IRDCs, Methanol Masers, IR bubbles and Star-less clumps. A rough size of the filamentary star forming region is measured on each $5.8 \mu\text{m}$ image using ruler option on the SAOIMAGE DS9 image display widget. The approximate size (in arc minutes), as well as the distances assumed for each region (refer Sec. 3.3) are also tabulated in Table 1. It is seen that the number of Class I sources roughly scales with the number of star-less clumps.

The estimated mass distributions of Class I and Class II sources in the identified 10 regions are shown in Figure 5. The histograms presented in Figures 5 and 6 may be hugely influenced by an incomplete census of YSOs. This study is likely to have missed a number of low mass objects, and they are more sensitive to (low mass) Class II objects than Class I objects. It can be seen that Class I sources are found to have a range in mass with most of them having mass $\geq 8M_{\odot}$. The upper mass limit in most of the region is found to be 30 - $32M_{\odot}$, though there are a few massive sources. The most massive YSOs in our study are found in regions 5 and 6. Among the Class I sources, 8 sources have estimated mass $> 30M_{\odot}$; 4 of them are in region 3, 1 source is in region 4, 2 are in region 5 and 1 source in region 6. 6 of them are in the mass range 30 - $36M_{\odot}$; while 2 in the 48 - $50M_{\odot}$; the latter being the most massive ones in this study. These suggest that the region studied here are indeed forming massive stars. Region 5 has the highest ratio of massive Class I to Class II sources. Regions 1 and 2 are found to have more low-mass sources, whereas region 6 has more sources in the high-mass range.

The mass distribution shows that for all the regions there is significant reduction in the number of Class II sources with mass higher than $8M_{\odot}$; while most of Class I sources have masses more than $8M_{\odot}$. Number of Class I sources in the mass range, $< 6M_{\odot}$ is relatively less; where we can see enough number of Class II sources. This may not be due to lack of Class I sources with $< 6M_{\odot}$ mass, but due to the detection limit. Observational evidence for lower-mass protostars is difficult to obtain. As high-mass protostars are much more luminous than lower mass protostars, they are far easier to detect. In Class II phase we do find higher fraction of lower mass protostars, as it becomes more identifiable in this phase. Region 1 is found to have relatively large number of low-mass Class I sources and it may be due to the fact that this region is relatively closer, as being part of the M17SWex.

The estimated age distributions of Class I&II sources in the identified 10 regions are shown in Figure 6. Most of the Class I and Class II sources are with age ≤ 0.1 Myr. In all regions, Class II sources have larger range in age, with some sources as old as 3 Myr. The age distribution for Class II sources shows that in some regions star formation started at ~ 3 Myr back, it continued till the Class I and Class II are formed together in the recent ≤ 0.5 Myr. Most of the Class I and II sources are found to be formed in the last 0.1 - 0.5 Myr. Regions 1, 3 and 6 show a more or less continuous formation of Class I sources with ages upto ~ 2.2 Myr.

3.6 Star formation in Filaments & clusters

The description of 8 filamentary star formation sites and 2 candidate clusters of Class I and Class II objects including their

observed structural details, YSO content, age and mass distributions of YSOs and other sources associated are given below.

1. G14.2-0.55 (Region 1 - Figure 7)

This region is a part of M17SWex which extends ~ 50 pc southwest from Galactic HII region M17. Povich & Whitney (2010) carried out the census of young stellar content using 2MASS, GLIMPSE, MIPS GAL and MSX data and detected > 200 YSOs which form B stars. For the 64,820 GLIMPSE sources located within a $1^{\circ} \times 0.75^{\circ}$ field encompassing M17SWex, Kurucz (1993) reddened stellar atmospheres were fitted and those sources with poor fit are considered as possible YSOs by Povich & Whitney (2010). From these, sources with IR excess emission were filtered out using Smith et al. (2010) color criteria and AGB contaminants were removed by applying Whitney et al. (2008) color criteria. Assuming M17SWex will form an OB association with a Salpeter IMF, they suggested (1) more rapid circumstellar disk evolution in more massive YSOs and (2) delayed onset of massive star formation in this region. We do not study the entire M17SWex region, but a major part of filamentary dark clouds, which are termed as region 1 and region 2. Our study tries to look at the general trend in mass and age for YSOs which are being detected in or near the filamentary dark clouds.

Distribution of Class I sources follow the pattern identical to that of the structure of dark filaments giving the impression that both are co-located; while most of the Class II sources are not closely associated with the filamentary structure. Instead of a single elongated hub, many tiny filaments are oriented in the decreasing longitude direction (away from M17) giving the appearance of an elongated dark filament. For a distance of 2.1 kpc (Povich & Whitney (2010)) we estimate a length of ~ 12 pc for this filament corresponding to $20'$ size. Class II sources show a peak in mass at around 2 - $3M_{\odot}$ and Class I sources peak at 8 - $9M_{\odot}$. Class I sources also show a distribution in mass upto 15 - $20M_{\odot}$; while Class II sources have masses only upto $10M_{\odot}$. From the age distribution of Class I and Class II sources, it can be seen that most of sources are formed at ≤ 0.1 Myr. Some of the Class II sources have ages upto 2 Myr; while most of the Class I sources have age ≤ 0.2 Myr. The star formation processes are found to have started around 2 Myr ago as evident from the presence of almost 10 Class II sources as old as 2 Myr (Figure 6). The star formation has continued and has produced a maximum number of both Class I and Class II sources forming together at about 0.1 Myr ago. As suggested by Povich & Whitney (2010), we also detect an increased formation of YSOs, after a delay of ~ 2 Myr in this region.

2. G13.87-0.48 (Region 2 - Figure 8)

This region is also a part of M17SWex and has been studied by Povich & Whitney (2010). For the distance of 2.1 kpc towards this region we estimate a length of ~ 8.5 pc for this filament corresponding to the $14'$ size of the filamentary structure. Similar trends in the pattern of Class I and II sources noticed in region 1 are seen here. The distribution of mass of Class I/II sources does not show substantial difference from those noticed in region 1. Presence of elongated hubs can be seen here though the tiny filaments are not obvious. Here Class II sources started forming at around 1.6 Myr ago and star formation processes reached at its peak in the last 0.1 Myr with most of the Class I and Class II forming together. Thus we find that region 2 also has older Class II sources, but only younger Class I sources. Also Class II sources are found to be relatively younger than those in region 1, suggesting that the formation in region 2 started later, by about 0.4 Myr. This might support the suggestion of sequential star formation in the M17 complex.

3. G14.62-0.05 (Region 3 - Figure 9)

Table 1. Filamentary regions and clusters with their source content.

Region	Name	Distance		Class I	Class II	Number of			
		range* (kpc)	Size ($^{\circ}$)			IRDCs	Methanol Masers	IR bubbles	Star-less clumps
1	G14.2-0.55	4-6	20	59	57	27	1	-	4
2	G13.87-0.48	1.9-2.3	14	18	20	14	-	1	1
3	G14.62-0.05	1.9-2.3	-	71	54	40	5	3	13
4	G13.26-0.31	4-6	20	17	5	16	-	-	-
5	G13.05-0.15	4-6	33	163	32	40	1	1	~14
6	G12.8+0.50	4-6	-	21	36	21	1	1	5
7	G12.34+0.51	4-6	8	9	11	10	-	1	-
8	G11.86-0.62	4-6	7.5	7	6	8	1	-	-
9	G11.13-0.13	3.2-3.9	20	34	11	20	1	1	5
10	G10.67-0.21	4-6	9	26	9	20	3	-	1

* as given in the input of SED fitting tool (Refer sec. 3.1)

Along with IRDCs and starless cores, mid-IR nebulosity is also seen in this l - b range. We identify this region as a candidate cluster of Class I and II sources. Highly luminous background emission and absence of definite filamentary structure indicate that the region is more evolved than other regions. Class I sources are located mainly in the dark patches. Class I sources show a peak in the mass distribution at 8 - 13 M_{\odot} and ranges upto 30 M_{\odot} . The mass distribution of the Class II sources peaks at 5 - 6 M_{\odot} . No Class I source is seen with mass < 4 M_{\odot} . Only very few Class II sources have mass > 10 M_{\odot} ; where substantial number of Class I sources exist in the 10 - 30 M_{\odot} mass bin. Both Class I and Class II peak at the age \leq 0.1 Myr. Some of the Class II sources are relatively older, upto 2.1 Myr. Similar to the regions 1 and 2, this region also shows that most of the YSOs are formed about 2 Myr after the initial star formation. There exist 4 Class I sources with mass > 30 M_{\odot} in this region; with masses 30.74 ± 1.67 , 33.92 ± 0.45 , 34.49 ± 1.5 and 35.78 ± 10.75 , (in solar masses); the last one showing the highest error in estimated mass among all YSOs.

4. G13.26-0.31 (Region 4 - Figure 10)

The region consists of a network of tiny filaments, seen inclined to the general Galactic plane and parallel to region 5 which is located at a higher b value. Length of the structure is $\sim 20'$ which stretches from G13.15-0.38 to G13.4-0.24 and corresponds to a physical length scale in the range 23-34 pc for the adopted range of distance (4-6 kpc). The increased number of Class I sources above Class IIs suggests that this may be hosting a very recent star formation site. All Class I sources have age \leq 0.1 Myr; while Class II sources are mildly older, up to 0.3 Myr. Hence, unlike the regions 1 and 2, we detect only recent star formation activity in this region. Most of the Class II sources have mass in the range 3 - 5 M_{\odot} . More number of Class I sources are seen in 7 - 10 M_{\odot} and 13 - 14 M_{\odot} mass bins. This region also hosts a Class I source with mass $32.4 \pm 4.07 M_{\odot}$. This region is located close to W33, similar to region 5. Signatures of HFS with tiny filaments arising parallel to short axis of the hub are observed in this region. At some points the filaments are entangled together where more number of Class I sources are located. The formation of filaments in this region is likely to be created by the outflows/winds from W33.

5. G13.05-0.15 (Region 5 - Figure 11)

This is one of the prominent region which is located near the W33 complex, where we can see Class I sources closely associated with the filamentary structure. This is the longest filamentary structure with a size of $\sim 33'$ (corresponding to a physical length in the range 38-56 pc according to the distance adopted) located to the south-

east of W33 complex and is inclined with respect to the Galaxy plane. A long strand of dark filament with tiny filaments branching out at some points and entangled together at some points gives the impression of a hub-filamentary system.

The increased number of Class I sources over Class II sources and presence of large number of IRDCs along with the morphology of the filaments suggest that the region is highly primitive and harbors a stellar nursery. Comparatively evolved ultra compact HII region W33 complex should be influencing the structure as well as star formation in this region. The Class I sources are seen to be nicely aligned along the length of filaments which extends from G12.8-0.35 to G13.3-0.00 as seen in Figure 11. The mass distribution of Class I sources shows a peak at 9 - 10 M_{\odot} . Significant fraction of Class I sources have mass > 8 M_{\odot} indicating that this region is proliferately forming high mass stars. There are 2 Class I sources with mass greater than 30 M_{\odot} , with masses $30.74 \pm 1.06 M_{\odot}$ and $49.21 \pm 2.82 M_{\odot}$. Thus this region hosts the most massive YSO detected in this study. Only a very few Class II sources have mass higher than 10 M_{\odot} . It is found that both Class I and Class II have age \leq 0.1 Myr, with some of the Class II sources as old as 0.5 Myr. Similar to the star formation in region 4, this region also has started forming stars very recently.

6. G12.8+0.50 (Region 6 - Figure 12)

The region is abundant in Class II sources and dust lane emissions compared to other regions and is classified as a candidate cluster. This is the only region where we find significantly more number of Class II sources when compared to the number of Class I sources. Major fraction of Class II sources have mass in the 4 - 6 M_{\odot} range; while most of the Class I sources have mass upto 16 M_{\odot} , with a very few ranging upto 30 M_{\odot} . Class I sources have age \leq 0.1 Myr, where Class II sources are as old as 2.5 Myr. The Class II sources are found to be forming from 2.5 Myr till now, whereas the high mass stars are formed only now. The region hosts the second highest massive YSO detected in our study with a mass, $48.74 \pm 1.04 M_{\odot}$. The structure and star formation in this region is possibly modified by either the W33 region or the sites of star formation seen in dust emission.

7. G12.34+0.51 (Region 7 - Figure 13)

This region which has relatively faint features compared to other regions, consists of a filamentary structure with tiny filaments branching out forming a hub-filamentary system. The filaments can be seen emerging out of two regions which show dust emission, representing the hub. The filaments are found to be aligned in the same direction. The 8' size of this region corresponds to a length scale of

9 - 14 pc for the 4-6kpc adopted distance range. We detect only a few number of Class I & II sources in this region. Class II sources show a peak in mass in the range 5 - 6 M_{\odot} and Class I sources vary-ing upto 16 M_{\odot} . Both Class I and Class II sources have age \leq 0.1 Myr, but some Class II sources are as old as 1.8 Myr. As the Class I sources are not found in most part of the filaments, it appears that the filaments in this region has not attained the critical mass to start star formation.

8. G11.86-0.62 (Region 8 - Figure 14)

This region has the same pattern as that of region 7. Here also signatures of hub-filamentary system can be seen. Branching out of filaments to form a network is clearly observable in this region. Here also for the adopted distance range, we estimate a length of 8.7 - 13 pc corresponding to the 7.5' size of the filamentary structure. There are no Class I sources with mass $<$ 7 M_{\odot} and most of them have in the range 8 - 9 M_{\odot} . Masses of Class II sources vary from 2 - 11 M_{\odot} . Most of the Class I and Class II sources have age \leq 0.1 Myr. A few of the Class II have age 2.7 - 2.9 Myr.

9. G11.13-0.13 (Region 9 - Figure 15)

This is one of the well-studied filamentary IRDC. Carey et al. 1998 confirmed the presence of dense molecular gas in this cloud using millimeter spectral lines of H₂CO. Carey et al. (2000) presents the 850 μ m and 450 μ m continuum images from SCUBA observations and postulates the presence of early stages of star formation within the cloud. Johnstone et al. (2003) demonstrated the underlying radial structure of the cloud using 850 μ m observations and according to their findings this is the first molecular filament observed to have a radial profile similar to that of a non-magnetic isothermal cylinder. Henning et al. (2010) made use of Herschel data to detect the embedded population of pre- and protostellar cores in this. Out of 18 cores they characterized using SED analysis, two are of with masses over 50 M_{\odot} , implying the presence of massive star formation. The presence of high mass star formation in the cloud has been noted by other authors also; Chen et al. (2010) (presence of EGOs as a tracers), Pillai et al. (2006) (water and methanol emission), Gomez et al. (2011) (using methanol emission).

A distinct filamentary cloud structure with tiny filaments originating at some points is seen here. It is interesting to see that Class I sources are aligned along the string of filamentary structure; while Class II sources are located more or less away from the main filament. The approximate size of the filament is \sim 20'. This corresponds to a length of \sim 21 pc for the distance 3.6 kpc towards this region. Most of the Class I sources have mass $<$ 10 M_{\odot} and age \leq 0.1 Myr with a peak distribution in mass at 9 - 10 M_{\odot} and a very few ranges upto 30 M_{\odot} . Many Class II sources have mass in the range 5 - 9 M_{\odot} and age ranges to 0.5 Myr. Many IRDCs, star-less clumps (5 with near distance solution), one maser source and one IR bubble are seen in this location. IRDCs are also nicely aligned in these filaments. Most of the star formation in this region is found to be in the last 0.5 Myr.

10. G10.67-0.21. (Region 10) (Figure 16)

Tiny filaments emanating from smaller round hubs are grouped to make a clustered form of filaments in this region. This region with a 9' size corresponds to a length scale in the range 10 - 16 pc for the adopted distance range of 4 - 6 kpc. Most of the Class I and Class II have the age \leq 0.1 Myr. Masses of Class I sources vary upto 26 M_{\odot} with many peaking at 8 - 9 M_{\odot} . Class II sources have mass in the range 2 - 13 M_{\odot} . This is a site experiencing star formation in the last 0.5 Myr.

4 DISCUSSION

We have studied YSOs in 10 star forming regions in the inner Galaxy. The presence of massive Class I sources along with other tracers of high mass star formation prove that these are sites of high mass star formation. The regions show filamentary dust lanes and Class I sources are found to be preferentially located along them. As these regions are located near the well-known HII regions, the structure and star formation in these regions may be dictated by them.

Figure 17 shows the location of tracers of high mass star formation such as IRDCs, masers, star-less clumps, IR bubbles/HII regions, radio sources, EGOs and HMPOs identified in the galactic region of our study. Though the 10 regions studied here are selected based on the density of the Class I and Class II sources, a few other concentrations of above mentioned tracers can be identified in this plot. Thus, figure 17 shows the location of these concentrations and suggests that there may be a few more high mass star forming sites, close to the regions studied here. We do not study them as we detect only a few Class I sources in these regions. It is possible that these regions are in the very early stage of star formation. Presence of such regions once again strengthens the argument that this region of the Galaxy is undergoing high mass star formation, which are potential targets for further studies.

Out of the 10 regions studied here, 4 regions (regions 1, 2, 3 and 6) show signatures of delayed star formation. Though our results suggest a delay in the formation of Class I sources (massive stars), this is only indicative because of the incompleteness in the data of Class II sources. Regions 1, 2 and 3 are located close to M17SWex. There is indication of sequential star formation in this region due to the effect of M17SWex. 6 regions (regions 4, 5, 7, 8, 9 and 10) were found to be forming the high and low mass stars together. Stars are being formed in these regions in the last 0.5 Myr.

Figure 18 shows the plot of age vs mass for the Class I and Class II sources with estimated errors in masses and ages. In the plots we have truncated the limits in both X and Y axes, including most of the sources; while excluding the extreme ones. The interpretations of this plot are likely to be affected by the incomplete number of observed YSOs in the region. Also, errors on many of the masses and ages are greater than the predicted values themselves. In the case of Class I sources, the plot is shown only upto 1 Myr, though there are 13 sources with ages more than 1 Myr and upto 8 Myr having mass less than 8 M_{\odot} . It is possible that these older Class I sources may be Class II sources viewed edge-on, through their disks. Most of the Class I sources detected in the regions are found to be younger than 0.5 Myr and this plot helps to understand the mass distribution of this population.

The mass of Class I sources were found to be between 2 - 32 M_{\odot} , with most of the sources more massive than 8 M_{\odot} . Thus, high mass stars are being formed in these regions in the last 0.5 Myr. It can be seen that the relatively low mass Class I sources have age upto 0.5 Myr, whereas the more massive sources are younger than 0.2 Myr. It is well known that massive stars form much quicker than their low-mass counterparts. One would therefore not expect to see massive Class I sources with ages greater than a few tenths of a Myr. The left-hand plot in Figure 18 supports this theory. The Class II sources are formed in the age range 0 - 3 Myr, but most of the sources have ages \leq 0.6 Myr. There are about 20 sources which are older than 3 Myr, up to 10 Myr and having masses less than 5 M_{\odot} . This suggests that most of the Class II sources have similar age range as the Class I sources. The mass range of the Class II sources is found to be 0.5 - 20 M_{\odot} , but most of the sources have

mass less than $10 - 12M_{\odot}$. Most of the older Class II sources were found to have mass less than $8M_{\odot}$, except a few massive sources. The above numbers are only suggestive and could be affected by the incompleteness in the data. We do still find that many - in some regions most - of the Class II sources appear to be as young as the Class I sources. This can be either due to observational bias towards massive YSOs which evolve more rapidly than their low-mass counterparts or some of the class II sources are mis-identified as Class I in the colour-colour analysis because of their orientation (i.e., being viewed pole-on). The environment around each sources, orientation of the source with respect to the observer and the mass of the central object can alter the observed differences in colours and SEDs of Class I and Class II evolutionary stage objects thereby affecting the properties estimated for them and can be the reason for obtaining large population of very young Class II sources. Apart from these biases in the classification of the YSOs, this study supports the evolution of Class I sources into Class II sources.

In summary, we detect YSOs in the mass range $0.5 - 31M_{\odot}$ and $\sim 0.1 - 3$ Myr age range, with most of them in the ≤ 0.5 Myr age range. These regions, thus prove to be abundant in massive YSOs in the early stages of formation, pointing to their potential for further studies. One of the regions studied here is found to have a large number of high mass Class I sources, suggesting that this region (region 5) is forming a massive and rich cluster of high mass stars.

We observe HFS in most of the early star forming complexes of filamentary IRDCs. In most cases elongated hubs are seen with tiny filaments. We see different orientations of filaments with respect to the central hub, like, the filaments parallel to hub, filaments radiating in different directions, and in some cases filaments are entangled. Myers (2009) explains the different models of formation mechanism of HFS. Analysis of each filamentary star formation sites and their environment can lead to the understanding of formation scenario of HFS. The filamentary regions are located in the vicinity of massive HII regions, suggesting that the filamentary features could be created due to these nearby HII regions. Our regions are located at varying distances from the HII regions and some are located relatively far away. Also, some of these regions are found to host star formation upto 3 Myr ago, with the formation of low mass stars. Thus, the early formation of small number of low mass stars is not found to destroy the filaments.

Studies of star formation in filamentary structures is an upcoming area of scientific interest as the new space missions like Herschel and other sub millimeter observations have recently shown the complex systems of filamentary structures. These informations have revolutionized the previous theory of star formation that only self accreting molecular clouds of circular size take part in star formation. We have shown that the GLIMPSE data & images are enough to identify filamentary structures and thereby contribute in understanding the origin and geometry of early star forming processes.

5 CONCLUSION

Major findings of our study can be summarized as follows:

- We have identified 1107 Class I and 1566 Class II sources in the galactic region $10^{\circ} < l < 15^{\circ}$, $-1^{\circ} < b < 1^{\circ}$.
- We have identified 8 early star forming sites of filamentary structures and 2 candidate clusters of Class I and Class II YSOs. Class I sources are closely associated with the infra red dark filaments; while Class II sources are located randomly in these regions.

All these are found to be co-located with other high mass star forming tracers.

- In all the regions identified, the observed Class I sources are with age ≤ 0.5 Myr, while Class II sources have ages in the range $\sim 0.1 - 3$ Myr. Majority of the Class I sources are $\geq 8M_{\odot}$; while Class II sources in the $0.5 - 10 M_{\odot}$ mass range. Low mass objects are incomplete in this group due to low flux levels.

- 4 regions studied are found to show a delay in the formation of most of the YSOs. Our analysis supports the sequential star formation of M17SWex complex as suggested previously.

- Filamentary and hub-filamentary features are found in most of these regions, which harbor star formation in the $\sim 0.1 - 3$ Myr age range. The length of the identified filaments are estimated as $8' - 33'$ ($\sim 9 - 56$ pc).

- This study brings to focus 10 sites of massive star formation in the inner Galaxy, harboring very young YSOs. We suggest that these are potential targets to understand the formation and evolution of massive YSOs.

6 ACKNOWLEDGMENTS

We thank the anonymous referee for the useful comments and suggestions which helped in improving the paper. BB gratefully acknowledges University Grants Commission, New Delhi, for financial support through RFSMS Scheme and Indian Institute of Astrophysics, Bangalore, for hospitality, where most of this work was done. This research has made use of the data products from the GLIMPSE survey, which is a legacy science program of the Spitzer Space Telescope funded by the National Aeronautics and Space Administration and also the data products from Two Micron All Sky Survey (2MASS), which is a joint project of the University of Massachusetts and the Infrared Processing and Analysis Center/California Institute of Technology, funded by the National Aeronautics and Space Administration and the National Science Foundation.

REFERENCES

- Anderson, L. D.; Bania, T. M.; Balser, Dana S.; Rood, Robert T., 2011, ApJS, 194, 32A
- Beltran, M. T., Cesaroni, R., Neri, R., Codella, C., 2011, A&A, 525, 151
- Benjamin, R. A., Churchwell, E., Babler, B. L., 2003, PASP, 115, 953
- Bernasconi, P. A., & Maeder, A. 1996, A&A, 307, 829
- Beuther, H., Linz, H., Henning, Th., 2011, A&A, 531, 26
- Carey, S. J., Clark, F. O., Egan, M. P., Price, S. D., Shipman, R. F., & Kuchar, T. A., 1998, ApJ, 508, 721
- Carey, S. J., Feldman, P. A., Redman, R. O., et al. 2000, ApJ, 543, L157
- Caswell, J. L., Murray, J. D., Roger, R. S., Cole, D. J. & Cooke, D. J., 1975, A&A, 45, 239
- Chavarria L. A., Allen L. E., Hora J. L., Brunt C. M. et al. 2008, ApJ, 682, 445
- Chen, X., Shen, Z., Li, J., Xu, Y., & He, J. 2010, ApJ, 710, 150
- Churchwell, Ed; Babler, Brian L.; Meade, Marilyn R., et al. 2009, PASP, 121, 213
- Clemens, D. P., Sanders, D. B., Scoville, N. Z., Solomon, P. M., 1986, ApJS, 60, 297
- Corbel, S., & Eikenberry, S. S., 2004, A&A, 419, 191

- Cyganowski, C. J.; Whitney, B. A.; Holden, E., et al. 2008, *AJ*, 136, 2391
- Dame, T. M., & Thaddeus, P., 2008, *ApJ*, 683, 143
- Downes, D., Wilson T. L., Beiging, J., & Wink, J., 1980, *A&AS*, 40, 379
- Ellingsen, S. P., 2006, *ApJ*, 638, 241
- Fazio, G. G., Hora, J. L., Allen, L. E., 2004, *ApJS*, 154, 10
- Flaherty, K. M., Pipher, J. L., Megeath, S. T., et al., 2007, *ApJ*, 663, 1069
- Furness, J. P., Crowther, P. A., Morris, P. W., et al., 2010, *MNRAS*, 403, 1433
- Gerin, M., de Luca, M., Goicoechea, J. R., et al., 2010, *A&A*, 521, 16
- Goldsmith, P. F. & Mao, X. J., 1983, *ApJ*, 265, 791
- Gomez, L., Wyrowski, F., Pillai, T., et al. 2011, *A&A*, 529, 161
- Goss, W. M., Matthews, H. E., & Winnberg, A., 1978, *A&A*, 65, 307
- Grave, J. M. C., & Kumar, M. S. N., 2009, *A&A*, 498, 147
- Green, J. A., McClure-Griffiths, N. M., Caswell, J. L., et al., 2009, *ApJ*, 696, 156
- Green, J. A., Caswell, J. L., Fuller, G. A., et al., 2010, *MNRAS*, 409, 913
- Gutermuth, R. A., Myers, P. C., & Megeath, S. T., 2008, *ApJ*, 674, 336
- Gutermuth, R. A., Megeath, S. T., Myers, P. C., et al. (2009), *ApJS*, 184, 18
- Haschick, Aubrey D., & Ho, Paul T. P., 1983, *ApJ*, 267, 638
- Henning, Th., Linz, H., Krause, O., Ragan, S., et al. 2010, 518, 95
- Jackson, J. M., E. T. Chambers, E. T., Rathborne, J. M., et al., 2008, *ASP Conf. Series*, 387
- Johnstone, D., Fiege, J. D., Redman, R. O., Feldman, P. A., & Carey, S. J. 2003, *ApJ*, 588, 37
- Kang, M., Bieging, J. H., Povich, M. S., & Lee, Y. 2009, *ApJ*, 706, 83
- Keto, Eric., 2002, *ApJ*, 568, 754
- Kim, Kee-Tae., Koo, Bon-Chul., 2002, *ApJ*, 575, 327
- Klaassen, P.D., Wilson, C.D., Keto, E.R., et al., 2011, *A&A*, 530, 53
- Kryukova, E., Megeath, S. T., Gutermuth, R. A., et al. 2012, *AJ*, 144, 31
- Kurucz, R. 1993, *ATLAS9 Stellar Atmosphere Programs and 2 km/s grid*. Kurucz CD-ROM No. 13. Cambridge, MA: Smithsonian Astrophysical Observatory
- Lada, C. J., et al. 2006, *AJ*, 131, 1574
- Liu, Haiyu Baobab., Zhang, Qizhou., & Ho, Paul T. P., 2011, *ApJ*, 729, 100
- Messineo, Maria., Davies, Ben., Figer, Donald F., et al., 2011, *ApJ*, 733, 41
- Myers, P. C. 2009, *ApJ*, 700, 1609
- Neufeld, D. A., Sonnentrucker, P., Phillips, T. G., et al., 2010, *A&A*, 518, 108
- Olmi, L., Cesaroni, R., Walmsley, C. M., 1996, *A&A*, 307, 5990
- Pascucci, I., Apai, D., Henning, Th., et al., 2004, *A&A*, 426, 523
- Peretto, N., & Fuller, G. A., 2009, *A&A*, 505, 405
- Persson, C. M., De Luca, M., Mookerjee, B., et al. 2012, *A&A*, 543, 145
- Pillai, T., Wyrowski, F., Menten, K. M., & Krgel, E., 2006, *A&A*, 447, 929
- Povich, Matthew S., Whitney, Barbara A., 2010, *ApJ*, 714, 285
- Purcell, C. R., Hoare, M. G., Cotton, W. D., et al. 2013, *ApJS*, 205, 1
- Rathborne, J. M., Jackson, J. M., Chambers, E. T., Simon, R., Shipman, R., & Frieswijk, W. 2005, *ApJ*, 630, L181
- Rathborne, J. M., Jackson, J. M., & Simon, R. 2006, *ApJ*, 641, 389
- Rathborne, J. M., Simon, R., & Jackson, J. M. 2007, *ApJ*, 662, 1082
- Robitaille, T. P., Whitney, B. A., Indebetouw, R., & Wood, K. 2007, *ApJS*, 169, 328
- Rolfs, R., Schilke, P., Zhang, Q., Zapata, L., 2011, *A&A*, 536, 33
- Rougeer, G. W., Oort, J. H., 1960, *PNAS*, 46, 1
- Sanders, D. B., Clemens, D. P., Scoville, N. Z., Solomon, P. M., 1986, *ApJS*, 60, 1
- Siess, L., Dufour, E., & Forestini, M. 2000, *A&A*, 358, 593
- Simon, R., Rathborne, J. M., Shah, R. Y., Jackson, J. M., & Chambers, E. T., 2006, *ApJ*, 653, 1325
- Smith, Nathan., Povich, Matthew S., Whitney, Barbara A., et al. 2010, 406, 952
- Soifer, B. T., Puetter, R. C., Russell, R. W., et al. 1979, *AJ*, 232, 53
- Sollins, Peter K., Zhang, Qizhou., Keto, Eric., & Ho, Paul T. P., 2005, *ApJ*, 624, 49
- Stern, D., Eisenhardt, P., Gorjian, Varoujan et al. 2005, *ApJ*, 631, 163
- Stier, M. T., Jaffe, D. T., Fazio, G. G., Roberge, W. G., et al., 1982, *ApJS*, 48, 127
- Tackenberg, J., Beuther, H., Henning, T., et al., 2012, *A&A*, 540, A113
- Werner, M. W., et al. 2004, *ApJS*, 154, 1
- Whitney, B. A., et al., 2008, *AJ*, 136, 18
- Wilson, T. L., 1974, *A&A*, 31, 83

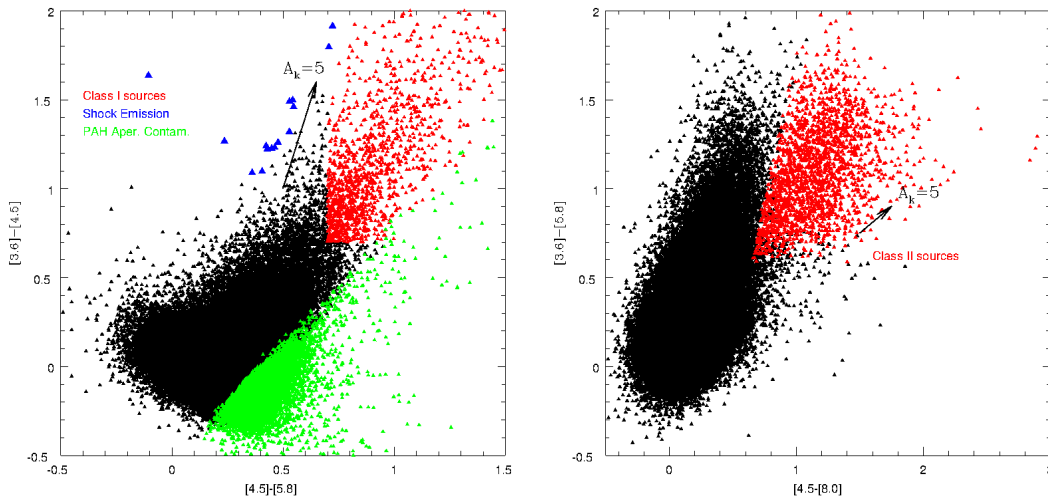


Figure 1. IRAC color-color Diagrams showing YSOs and non-YSO sources. *Left:* Shock emission sources as blue triangles, PAH aperture contaminants as green triangles and Class I sources as red triangles. *Right:* Class II sources as red triangles. Unclassified sources as shown as black triangles in both figures. Extinction vector corresponding to $A_k=5$ mag is shown.

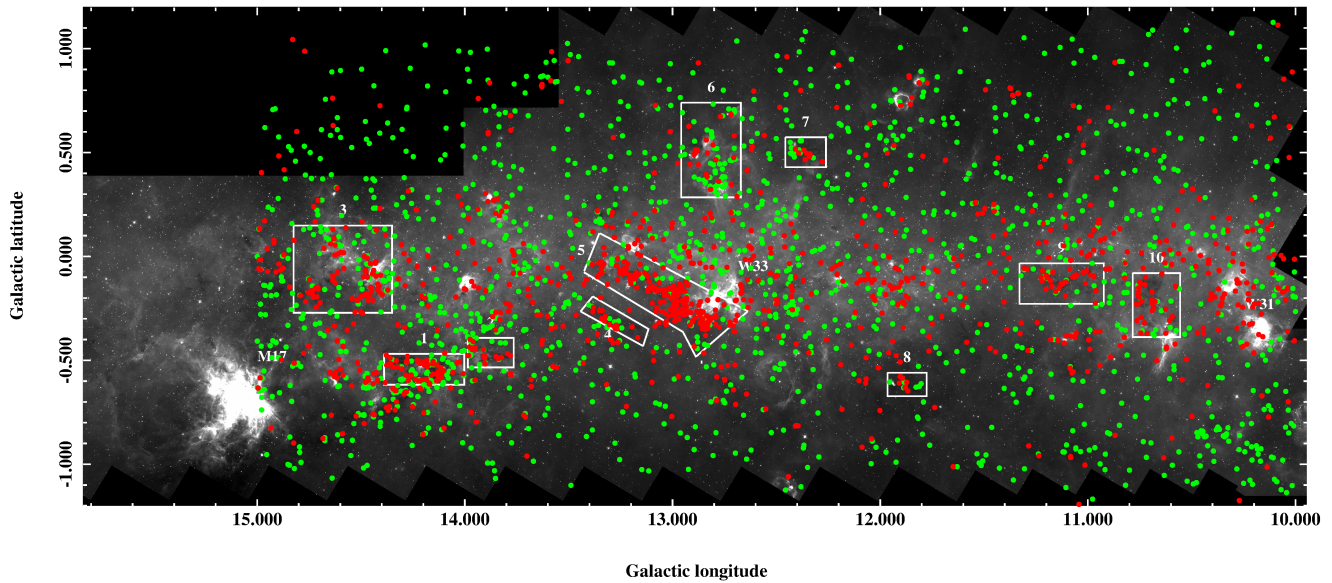


Figure 2. The region of our study as seen in the GLIMPSE $5.8\mu\text{m}$ image. X-axis is Galactic longitude, l and Y-axis is Galactic latitude, b . Distribution of Class I sources (red points) & Class II sources (green) in the region are shown. Regions marked inside the white boxes are the identified star formation sites. Location of M17, W33 and W31 are also shown.

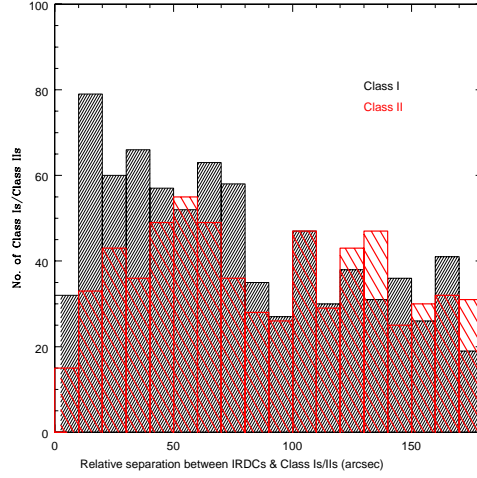


Figure 3. Histogram showing the relative separation of IRDC centres and Class I/II sources. More number of Class I sources are associated with IRDCs than Class IIs for smaller angular separations.

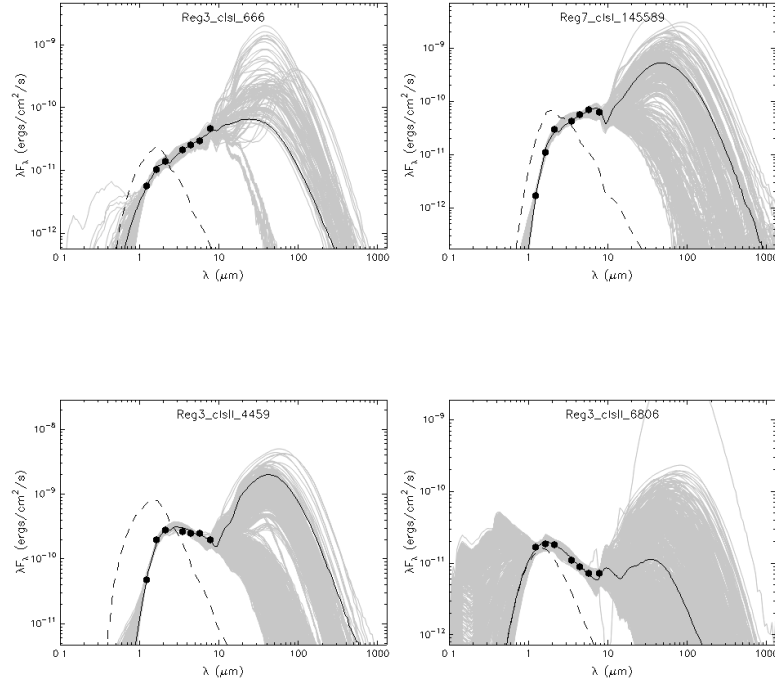


Figure 4. SEDs of Class I and Class II sources constructed using JHK_s and IRAC magnitudes. The top 2 sources are the Class I sources from region 3 and region 7 with ages 0.004 ± 0.068 Myr, 0.014 ± 0.075 Myr and masses $2.09 \pm 0.3M_{\odot}$, $7.14 \pm 0.04M_{\odot}$ respectively. Bottom sources are Class II sources from region 3 with ages 0.469 ± 0.074 Myr, 0.013 ± 0.041 and masses $4.89 \pm 0.03M_{\odot}$, $10.4 \pm 0.05M_{\odot}$ respectively.

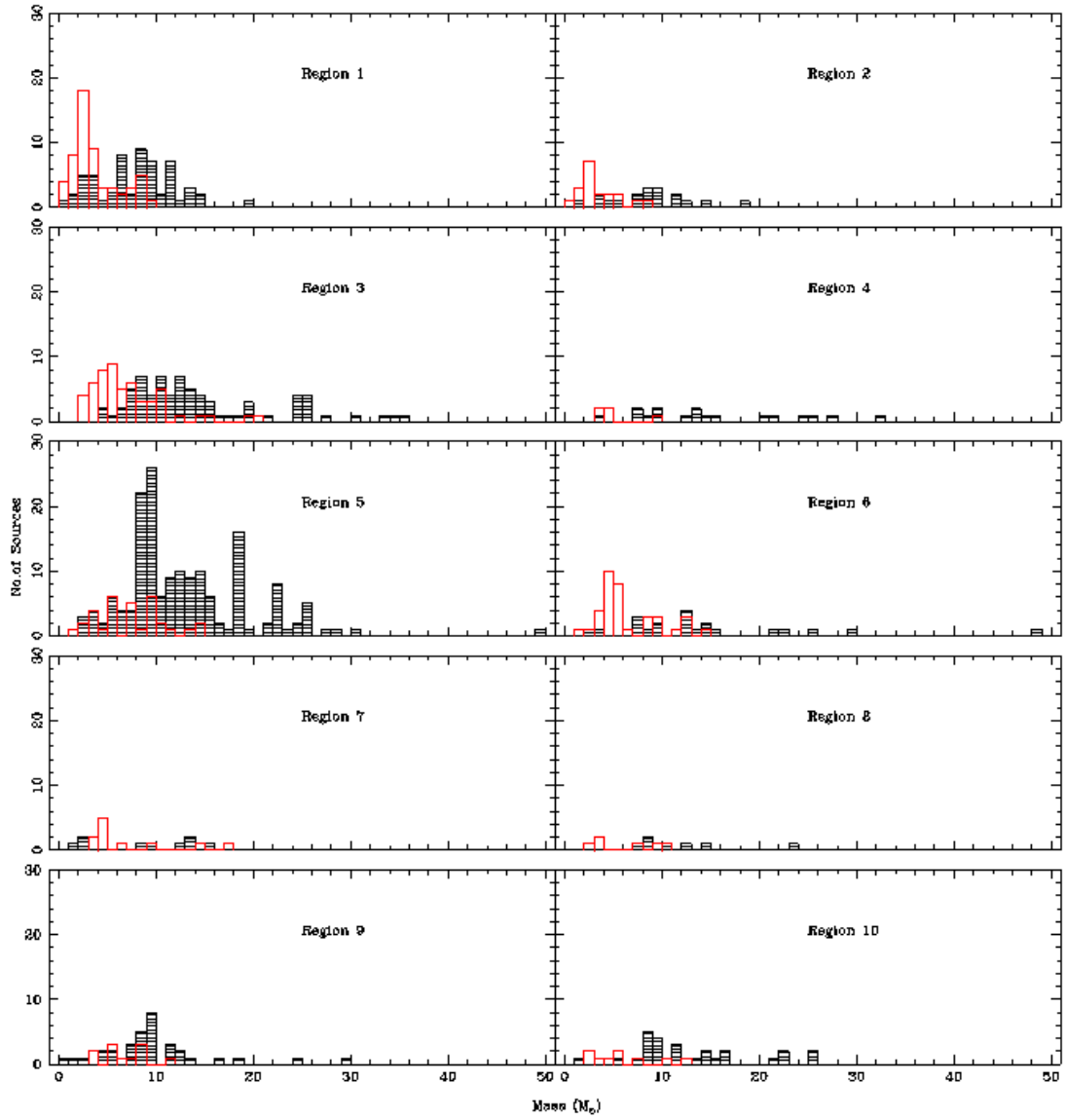


Figure 5. Mass distribution of Class I sources (black shaded blocks) and Class II sources (red blocks) identified in 10 regions.

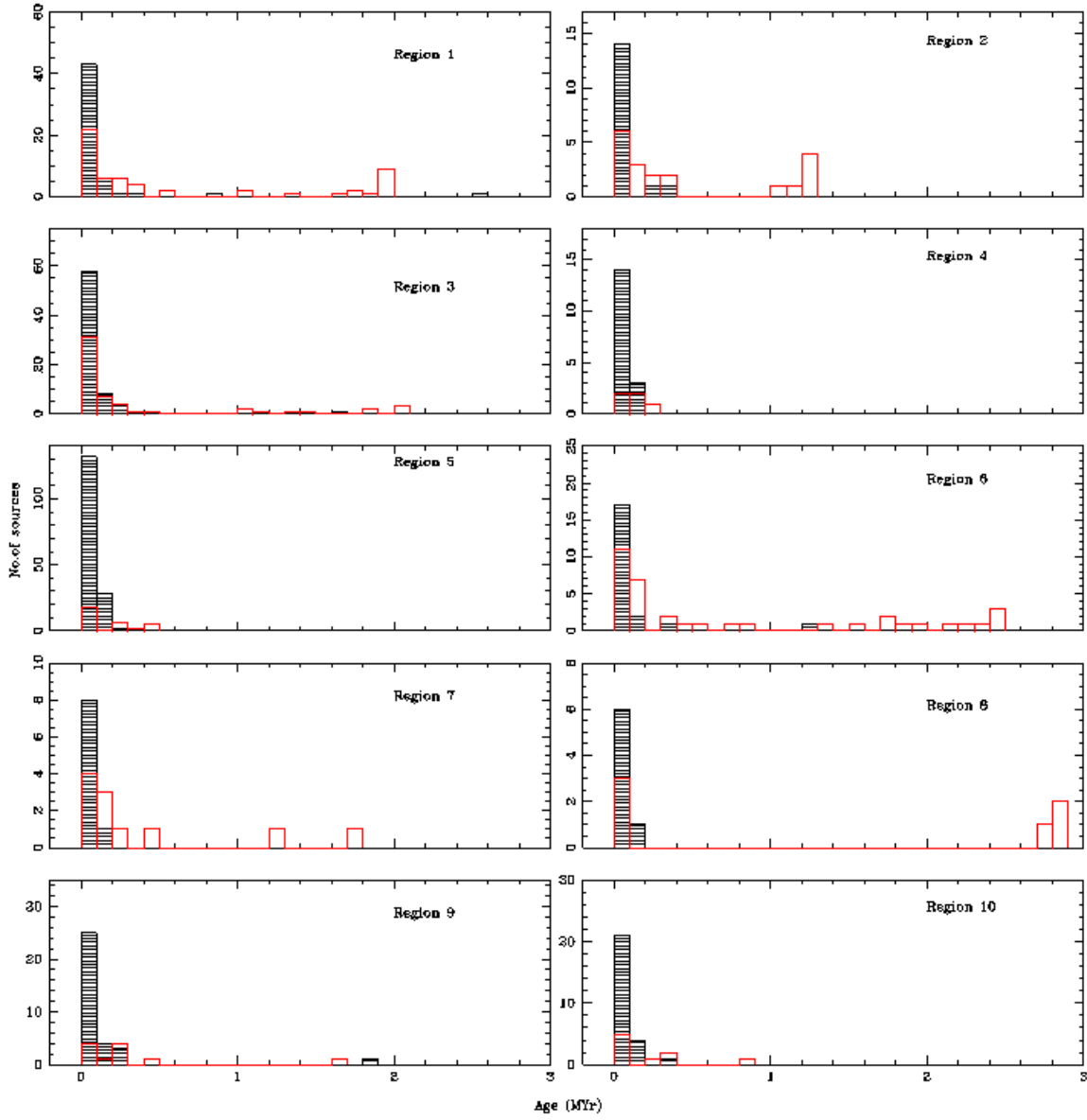


Figure 6. Age distribution of Class I sources (black shaded blocks) and Class II sources (red blocks) identified in 10 regions.

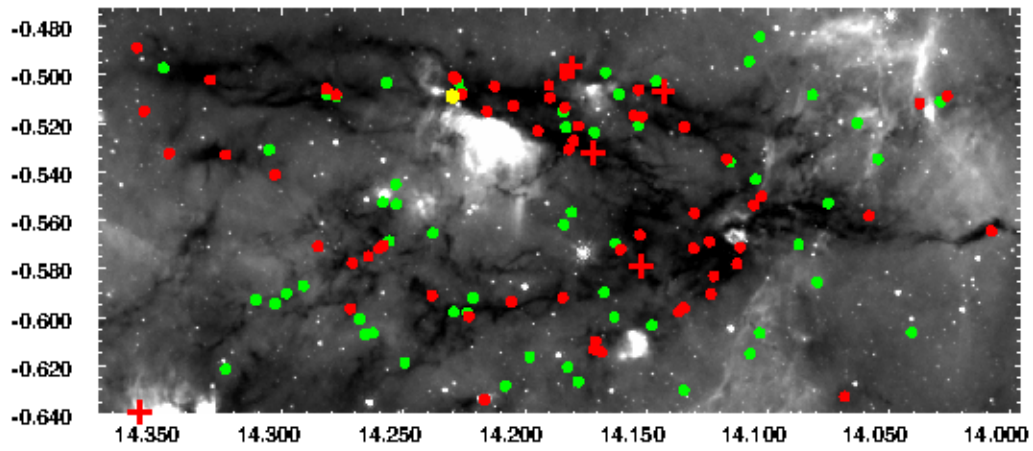


Figure 7. G14.2-0.55 (Region 1). Class I sources are shown in red circles and Class II sources in green circles. Only those YSOs considered for SED fitting are shown. Location of tracers like, Masers, star-less clumps are also marked. Yellow:Masers (without distance information), Blue:Near 3-Kpc arm Masers, Magenta:Far 3-Kpc arm masers, Red crosses: Star-less clumps with near distance solutions assumed, Red diamonds: Star-less clumps with far solutions.

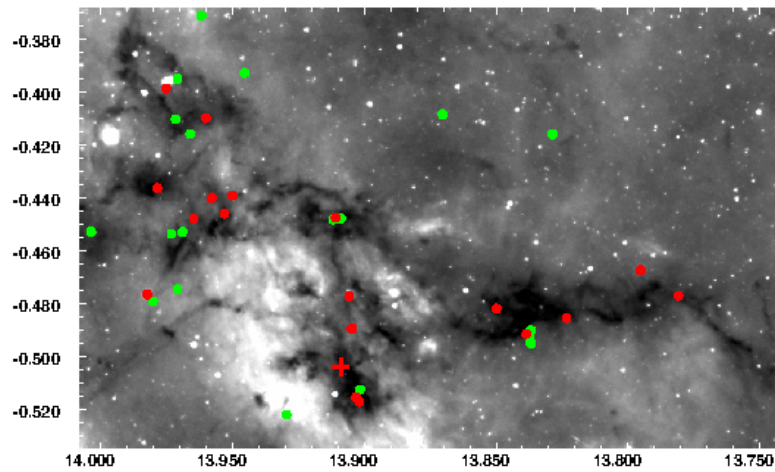


Figure 8. G13.87-0.48 (Region 2)

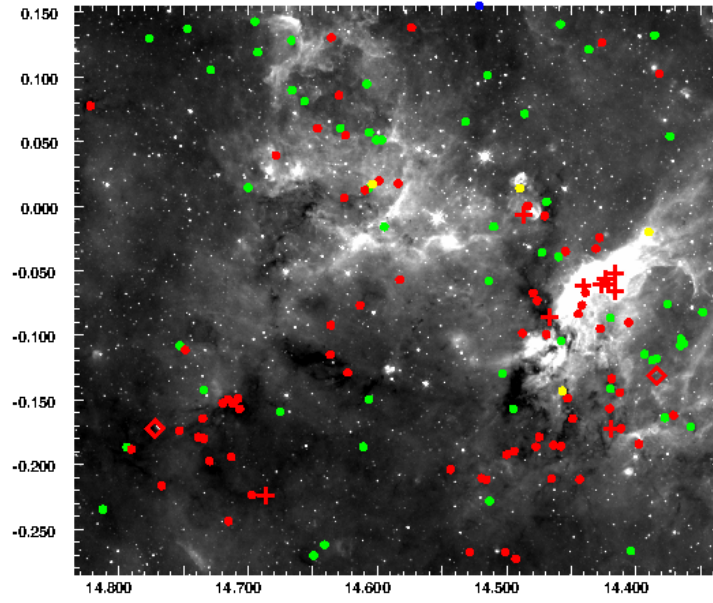


Figure 9. G14.62-0.05 (Region 3)

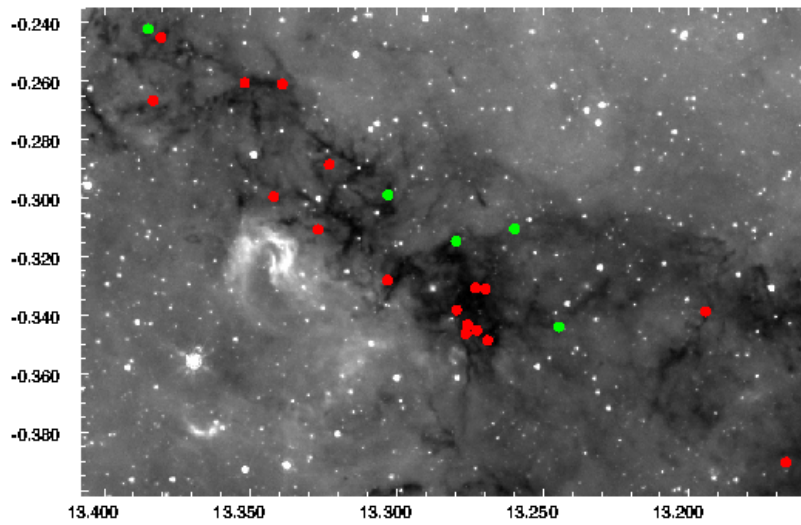


Figure 10. G13.26-0.31 (Region 4)

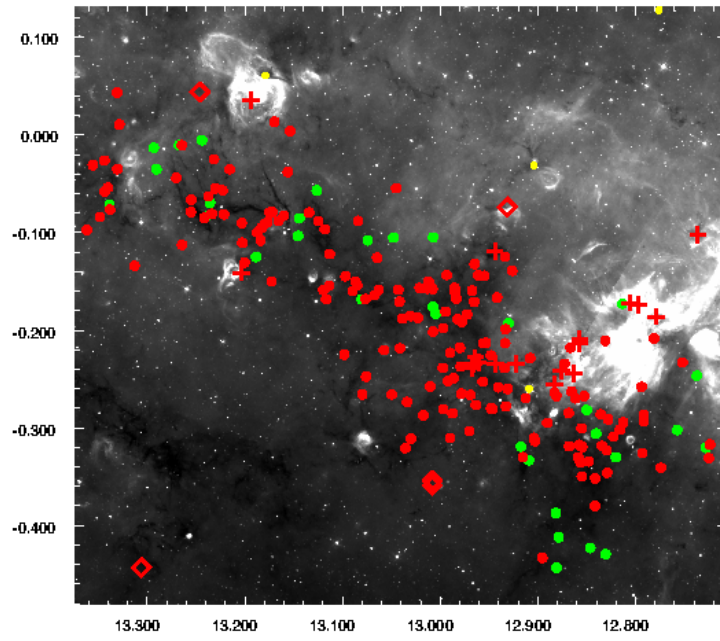


Figure 11. G13.05-0.15 (Region 5)

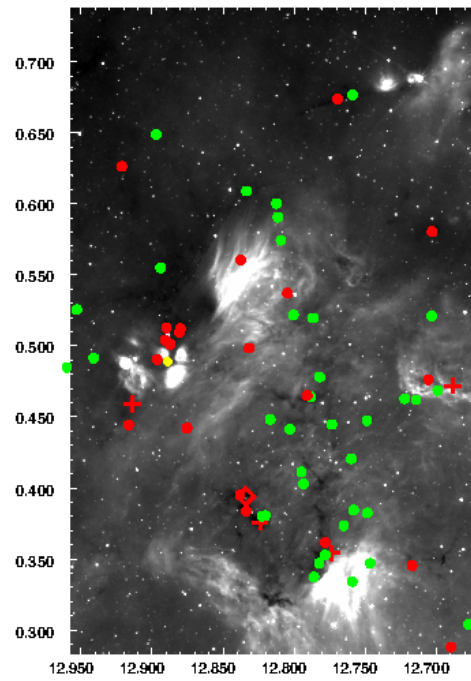


Figure 12. G12.8+0.50 (Region 6)

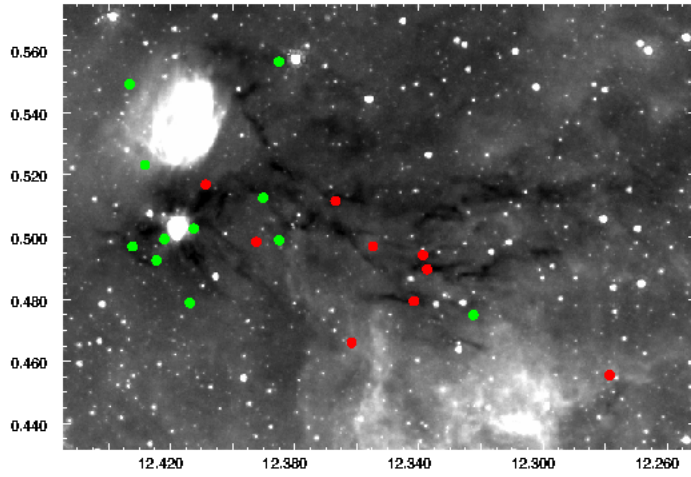


Figure 13. G12.34+0.51 (Region 7)

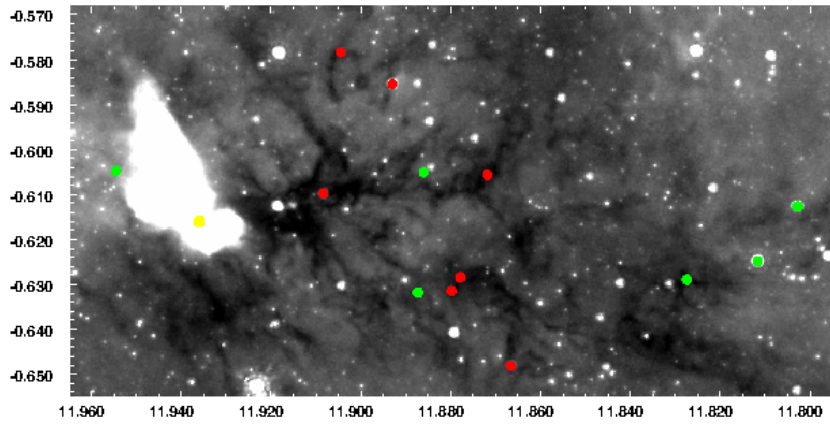


Figure 14. G11.86-0.62 (Region 8)

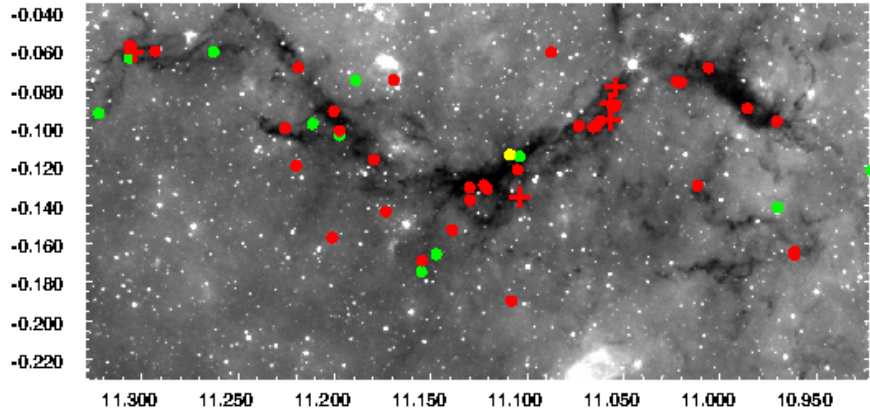


Figure 15. G11.13-0.13 (Region 9)

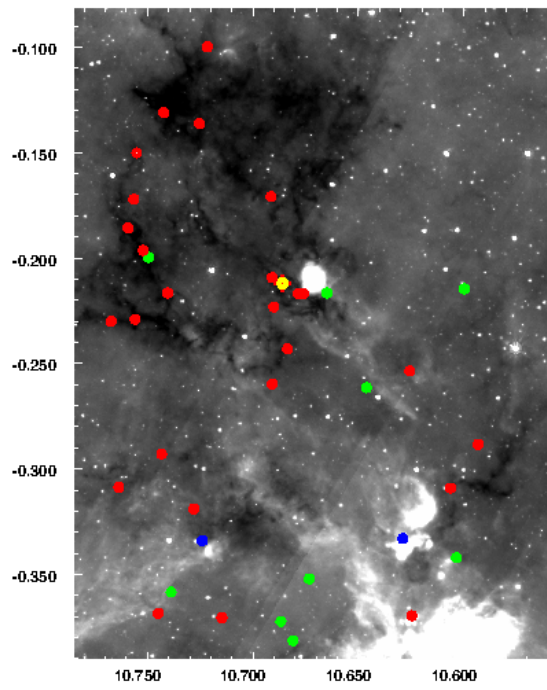


Figure 16. G10.67-0.21 (Region 10)

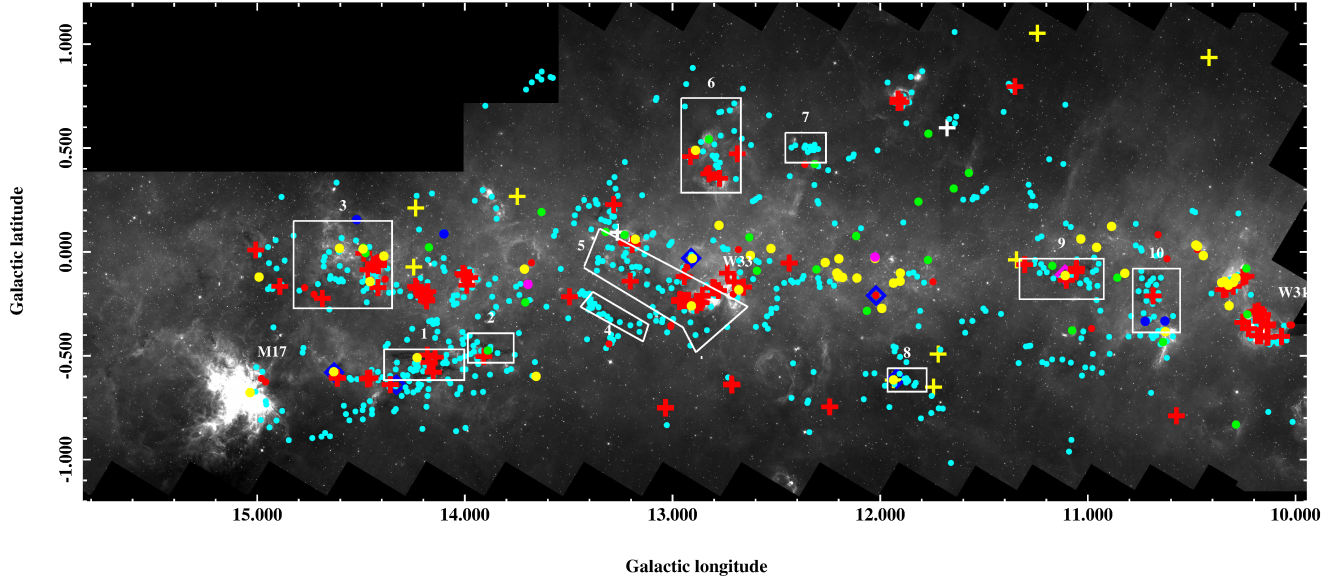


Figure 17. GLIMPSE 5.8μm image of entire region with the location of sources which are used as tracers of massive star formation and distance informations in our study. Circles:- Cyan:IRDCs, Green:IR bubbles/HII regions, Yellow:Masers, Blue:Near 3-Kpc arm Masers, Magenta:Far 3-Kpc arm masers, Red crosses: Star-less clumps with near distance solutions assumed, Red circles: Star-less clumps with far solutions, Blue diamonds:'likely' MYSOs, Magenta diamonds:'possible' MYSO, White crosses:HMPOs, Yellow crosses:Radio sources

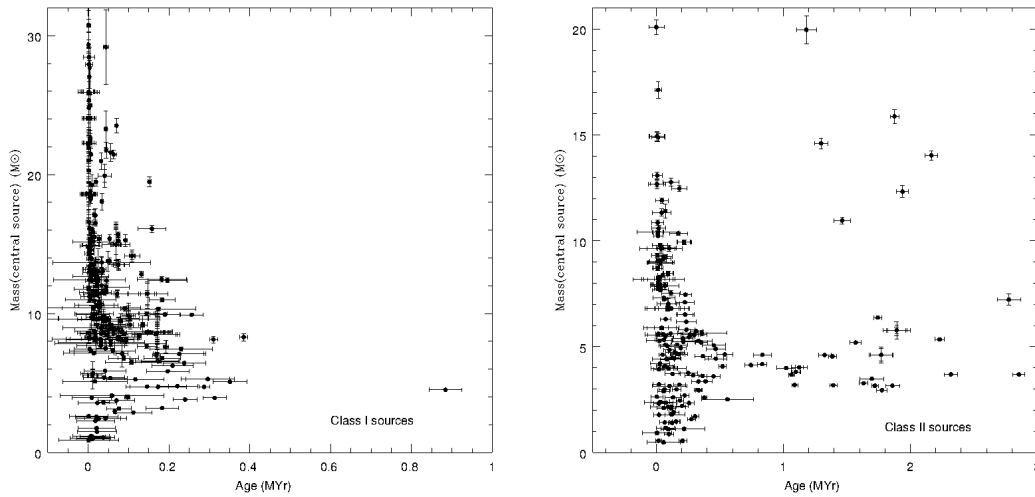


Figure 18. Mass and Age distribution of sources in the entire region. The central black dots correspond to the estimated mass and age of each of the YSOs. Std. deviations in estimated age and mass are shown as vectors along X axis and Y axis respectively.